

Specific Heat of Granular Aluminum Films*

R. L. Greene,[†] C. N. King, and R. B. Zubeck

Department of Applied Physics, Stanford University, Stanford, California 94305

and

J. J. Hauser

Bell Telephone Laboratories, Murray Hill, New Jersey 07977

(Received 31 March 1972)

The specific heat of granular Al-Al₂O₃ films with $T_c \cong 2^\circ\text{K}$ has been measured between 1.3 and 8°K. The results show that the enhancement of T_c is a bulk effect. Within experimental accuracy the electron density of states at the Fermi surface is the same as that of pure Al. The lattice heat capacity is increased in the granular films such that the measured Θ_D is 28% less than that of pure Al. This result indicates that the phonon density of states is greatly enhanced at low frequencies and seems to confirm the tunneling data of Klein and Leger. The experimental methods used to measure the small (~ 0.5 erg/°K) heat capacity of the films are discussed. The thermal conductivity of Au+7-at.-%-Cu wire and the heat capacity of silicon (~ 50 mg) were measured to test the capability and accuracy of the experimental techniques.

I. INTRODUCTION

Since the pioneering experiments of Buckel and Hilsch,¹ the transition temperature of Al and other superconductors has been enhanced by a variety of methods.² Such techniques as evaporation onto a 4.2°K substrate, evaporation with a partial pressure of oxygen, or coevaporation of metal atoms and other atoms, all produce small-grain-size (granular) films with an enhanced T_c . For Al the enhanced T_c can be as high as 6.45°K, though more typically 2°K, as compared to the bulk T_c of 1.19°K.

Numerous theoretical studies have tried to explain the enhancement of T_c in superconducting films. Although no one theory has explained all the experimental results, most experiments on nontransition metals are compatible with McMillan's³ idea that the occurrence of "soft" phonon modes can lead to higher T_c . For example, Leger and Klein⁴ explained their tunneling results on the basis of soft *surface* phonons being responsible for the enhanced T_c in granular Al films.⁵ On the other hand, one of the authors² has found that the enhancement of superconductivity in granular Al films can be explained by a shift in the bulk-phonon spectrum associated with an increase in atomic volume. This explanation is consistent with McMillan's model without having to invoke the concept of surface phonons.

In order to better understand the enhancement of T_c we have for the first time measured the low-temperature specific heat of a granular Al film.⁶ From the specific heat we can determine and compare to normal Al two important parameters in superconductivity theory, namely, the electron density of states at the Fermi surface $N(0)$ and the

lattice Debye temperature Θ_D . Any change in Θ_D from the normal value will be related to changes in the phonon density of states. In addition, the heat capacity, being a bulk measurement, can show if the enhanced T_c is a property of the entire film. The previous resistive and tunneling experiments were subject to uncertainty due to possible surface and filamentary effects.⁷

Whereas previous workers⁸ have used the ac technique to measure very small, almost discontinuous, *changes* (0.015 erg/°K) in heat capacity, our experiment is a measure of the *absolute* heat capacity of the films from 1.5 to 8°K using both the relaxation-time⁹ and the ac method.¹⁰ Our films have a heat capacity as small as 0.5 erg/°K. To our knowledge this is the smallest absolute heat capacity yet measured. The results of calculations describing the contribution of the finite heat capacity of the electrical lead wires to the experimentally measured heat capacity are presented. The performance of our apparatus was checked by measuring the heat capacity of a small silicon chip.

II. EXPERIMENTAL METHOD

A detailed description of the experimental techniques is given in Ref. 9. The basic configuration of the experiment is shown in Fig. 1. The sample, attached to a silicon thermometer, is inside a vacuum chamber and is thermally linked to a copper block by its two electrical leads. The copper block is brought to the desired temperature above the helium-bath temperature by means of an electrical heater and acts as a heat reservoir at that temperature. The sample and thermometer are heated above the block temperature by means of a He-Ne laser shining down a light pipe. Room-tempera-

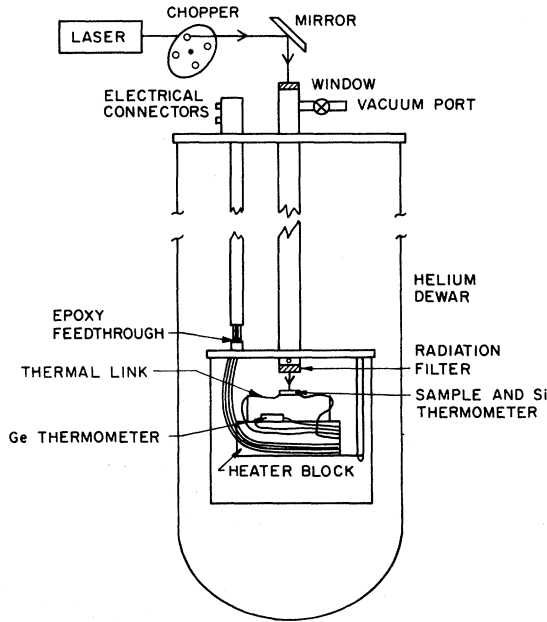


FIG. 1. Schematic diagram of experimental apparatus.

ture radiation is removed with an infrared filter¹¹ thermalized at the bath temperature. The rise in temperature of the sample is given by

$$\Delta T = T_{\text{sample}} - T_{\text{block}} = P/K_w, \quad (1)$$

where P is the power absorbed by sample and K_w is the thermal conductance of wire. This change in temperature is monitored by measuring the change in resistance of the silicon thermometer with an ac bridge.

Two different methods of determining the heat capacity were used. In the relaxation-time method the power is switched off and the ΔT decays exponentially to zero with time constant

$$\tau_1 = \frac{C_E}{K_w} = \frac{C_s + C_t + \frac{1}{3}C_w}{K_w}, \quad (2)$$

where C_E is the total experimentally measured heat capacity, C_s is the sample heat capacity, C_t is the thermometer heat capacity, and C_w is the wire heat capacity. As shown in Ref. 9, this represents the solution to the one-dimensional heat-flow equations in the case where τ_2 , the internal time constant for the sample, is much shorter than τ_1 . The heat capacity C_E is found from measuring τ_1 and K_w , i. e., $C_E = K_w \tau_1$.

The ac method involves supplying power to the sample at angular frequency ω and measuring the amplitude of the oscillating temperature of the sample at this frequency. In the ideal case where the inequalities $\tau_2 < 1/\omega < \tau_1$ are satisfied, the am-

plitude is related to the heat capacity by the formula¹⁰

$$|T(\omega)| = P(\omega)/\omega C_E. \quad (3)$$

We have shown elsewhere¹² that the finite heat capacity of the wire makes a contribution to C_E given by

$$C_E = C_s + C_t + C_w f(l/l_0), \quad (4)$$

where

$$f\left(\frac{l}{l_0}\right) = \frac{l_0}{2l} \left(\frac{\sinh(2l/l_0) - \sin(2l/l_0)}{\cosh(2l/l_0) - \cos(2l/l_0)} \right),$$

where

$$\left(\frac{l}{l_0}\right) = \left(\frac{\omega C_w}{2K_w}\right)^{1/2}.$$

The function $f(l/l_0)$ has the limiting forms

$$C_w f(l/l_0) \approx \frac{1}{3} C_w \quad \text{for } l/l_0 \lesssim 0.5, \quad (5a)$$

$$C_w f(l/l_0) \approx (l_0/2l) C_w \quad \text{for } l/l_0 \gtrsim 2. \quad (5b)$$

Thus, as the frequency increases (l/l_0 increases), a smaller fraction of the wire heat capacity contributes to C_E . Physically, this means that heat does not have time to flow as far down the wire during the shorter period of time $2\pi/\omega$. Note the quantity $f(l/l_0)$ is both frequency and temperature dependent. Therefore, a different fraction of C_w comes into C_E at different temperatures.

III. SILICON MEASUREMENT

As a test of our apparatus the heat capacity of a 50-mg silicon chip was measured from 1.5 to 10 °K. The silicon was n type with 1.7×10^{18} carriers/cm³ and is the same silicon that was used for our thermometers. One surface of the silicon chip was doped to be a resistance thermometer with two degenerate contact pads. Gold-copper alloy wire was bonded to the pads for electrical leads. The leads were 0.5 in. long and were either 0.003-in.-diam 22-carat gold-copper wire or 0.00125-in.-diam gold + 7-at.%-copper wire.¹³ Some of the experimental parameters of interest are shown in Table I.

Our temperature standard is a germanium thermometer calibrated by the CryoCal Company. The

TABLE I. Experimental parameters near 4 °K.

Parameter	Value
T	4.011 °K
τ_1	1.73 sec
f	26 Hz
$\omega \tau_1$	282
l/l_0	3.2
Silicon mass	47.947 mg

stated absolute accuracy of this temperature scale is $5 \text{ m}^\circ\text{K}$ from 2 to $5 \text{ }^\circ\text{K}$ and $10 \text{ m}^\circ\text{K}$ from 5 to $10 \text{ }^\circ\text{K}$. A confirmation of this temperature scale was made by comparing the CryoCal thermometer with a germanium thermometer calibrated with an ideal gas thermometer. Our temperature stability was $1 \text{ m}^\circ\text{K}$ over a period of 10 min . The temperature resolution was $0.5 \text{ m}^\circ\text{K}$. K_w is measured by self-heating the silicon resistance thermometer and measuring the incremental rise in temperature corresponding to the measured increment of power.

With our stability and resolution, temperature increments of 100 to $400 \text{ m}^\circ\text{K}$ were used to measure K_w to an accuracy of 2% . The measured thermal conductance is shown in Fig. 2. The data are fitted to the formula

$$K_w = AT + \frac{BT^2}{1 + CT^3} \quad (6)$$

This relation has been found to describe the thermal conductance of alloys.¹⁴ The first term is the electronic conduction and the second term represents the lattice conduction. It should be noted that the measurement of K_w determines the absolute accuracy of the experiment.

In Fig. 3 our data for silicon are plotted as C/T vs T^2 . Data were taken using both the relaxation-time and ac methods to verify that the contribution

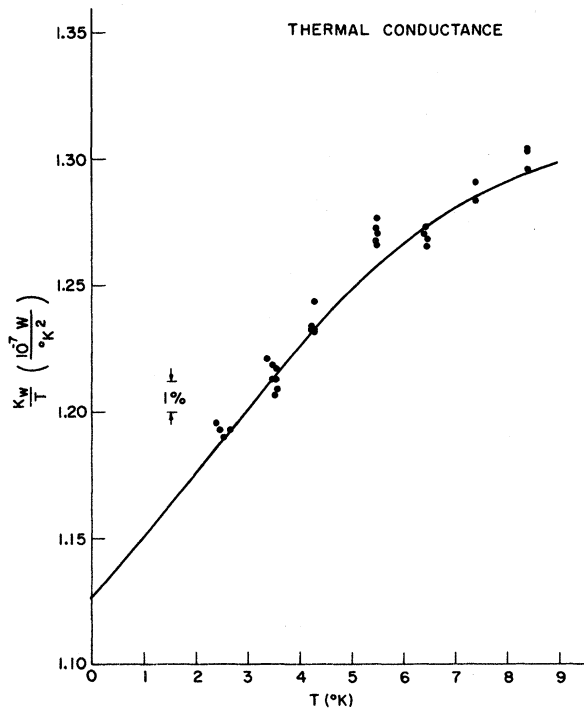


FIG. 2. Thermal conductance of Au + 7-at.-%-Cu wires. The thermal link consisted of two wires each 0.00125 -in. diameter and 0.5 in. in length.

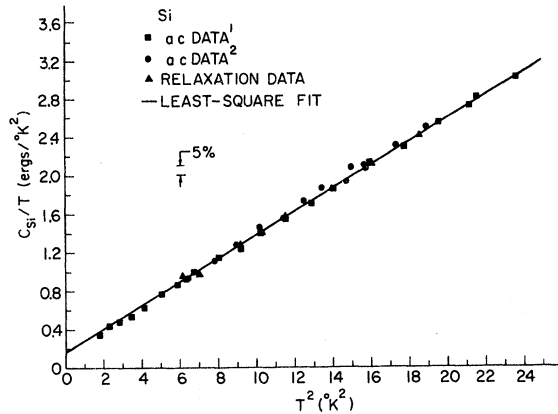


FIG. 3. Experimental heat capacity of 47.95 mg of silicon. The squares are data taken with 0.003 -in.-diam wires as the thermal links. The circles and triangles are data taken with 0.00125 -in.-diam wire.

of the finite wire heat capacity is correctly given by Eqs. (2) and (4). The first set of measurements was done using 0.003 -in.-diam wire, and the addendum heat capacity (gold contact pads and wire) was about 10% of C_E . The second set of measurements was done with 0.00125 -in.-diam wire, and the addendum was 5% of C_E . Within experimental error all of these measurements agree, verifying Eqs. (2) and (4). Most ac measurements were done at a frequency of 26 Hz . However, we also made measurements at 290 Hz to verify that there were no τ_2 effects. The heat capacity of the silicon chip was as small as $0.5 \text{ erg}/^\circ\text{K}$. The scatter in this data is $\pm 2\%$. The value of the Debye temperature we deduce from our data is $647 \pm 6 \text{ }^\circ\text{K}$. This is in good agreement with Flubacher, Leadbetter, and Morrison¹⁵ who found $\Theta_D = 645 \pm 5 \text{ }^\circ\text{K}$ with a sample of 150 g .

One feature of Fig. 3 may seem surprising. The finite value of C/T at $T=0$ implies that the silicon chip has electronic heat capacity. This heat capacity arises from the $10\text{-}\mu\text{m}$ -thick degenerate contact pads of the resistance thermometer. Using an estimated diffusion profile of the contact pads and data on the density of states at the Fermi surface as a function of n , we were able to calculate that the observed value of γ was of the correct size.

IV. GRANULAR ALUMINUM FILM MEASUREMENTS

Heat-capacity measurements were taken on a free-standing pure aluminum foil, a free-standing granular aluminum film, and a granular aluminum film sputtered onto the surface of a silicon thermometer. The temperature of the free-standing films was measured with attached thermocouples in contrast to the silicon thermometers used for the other measurements.

One set of samples was prepared by getter sputtering aluminum-aluminum oxide films onto the insulating faces of two 10-mg silicon thermometers and two sapphire slides.² The target was composed of 90-wt% Al and 10-wt% Al₂O₃. The substrate was at room temperature. The films were 25- μ m thick and took four days to deposit. The resistive T_c of the sapphire substrate film was 2.06 °K. Three days after deposition the residual resistivity was 160 $\mu\Omega$ cm, and the resistivity ratio was a metallic 1.09.

The films were analyzed for total aluminum content with an electron microprobe. Measurements were made at different accelerating voltages (5, 10, and 15 keV), with 15 keV corresponding to a 2.5 μ m penetration depth. Both Al metal and Al₂O₃ were used as reference standards. The films on silicon thermometers (B7, B8) were found to contain (84 \pm 2)-wt% Al. A chemical analysis¹⁸ on the film of sample B8 found (81 \pm 2)-wt% Al.

Using x-ray diffraction we found the films to be preferentially oriented with their [100] direction perpendicular to the substrate surface. By comparing the (200) line to 99.999%-Al powder sprinkled on the film surface, we found the d spacing to be $\frac{1}{2}\%$ larger than the pure Al, implying a volume expansion of 1.5%. The width of the x-ray lines indicated that the grain size was 250 Å.

In Fig. 4 a scanning electron micrograph of the granular aluminum film is shown. The surfaces of both film B8 and the film on a sapphire slide (No. 51) are composed of large granules of aluminum with diameters of \sim 5000 Å. Since this size is appreciably larger than the grain size determined by x-ray diffraction, the top 3 and then 9 μ m of film No. 51 were removed with an ion mill. After 3 μ m were removed the x-ray diffraction linewidths were increased, implying an average grain size of 160 Å; after 9 μ m the grain size was 100 Å. These data indicate that a range of grain sizes exists in these films with the larger grain sizes at the top film surface. The grain size in the interior of the films is probably as small as the 50 Å previously reported for thinner films.²

Three days after the sample was prepared the first set of heat-capacity measurements at low temperature was begun. To minimize the addendum we used 0.00125-in.-diam Au+7-at.%-Cu wires as electrical leads. The data from the first set of measurements are shown in Fig. 5. The upper points are measured total experimental heat capacity. The lower line represents the film heat capacity which is about 50% C_E near 4 °K. The data have 2% random scatter in C_E , and the absolute accuracy is \sim 3%.

A least-squares fit of the C_E data from 2.2 to 8 °K to the formula

$$C_E = \gamma T + \beta T^2 + \delta T^5 \quad (7)$$

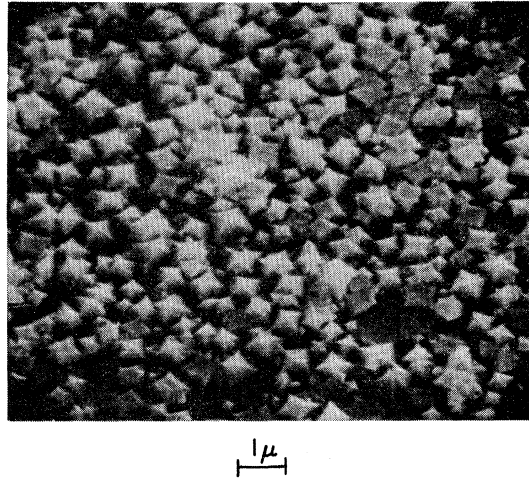


FIG. 4. Scanning electron micrograph of sample surface of film B8 as deposited. Magnification is 9000 \times .

gives the coefficients in Table II. Subtracting the addendum coefficients gives the film parameters.

The bump in the data near 2 °K is the superconducting transition. The sharp rise occurs between 2.05 and 1.95 °K which correlates well with the resistive transition at 2.06 °K. Figure 6 shows the details of the superconducting transition and the ideal BCS behavior for comparison. The transition is broad, extending down to at least 1.6 °K, indicating the film is most likely somewhat inhomogeneous. The area under data in Fig. 6 from $T=0$ to T_N ($T_N > T_c$) is the entropy at T_N . The second and third laws of thermodynamics demand that the entropy calculated in this way is equal to the entropy calculated from the normal-state heat capacity from $T=0$ to T_N . If the film is completely superconducting, the heat capacity of the film may be extrapolated to zero as the function $C_{film} \cong \alpha T^3$. The entropy calculated by using this extrapolation and the measured area under the data to 2.2 °K agrees with the entropy calculated from the normal-state heat capacity to within 5%. This implies that superconductivity is truly a bulk effect in these granular aluminum films. Furthermore, this provides a consistency check on the value of γ since it is the dominant factor in the entropy calculated from the normal-state heat capacity.

Two months after the first set of measurements, a second set was made to check the stability of the film. The resistive T_c of the film on the sapphire slide was the same within 0.01 °K. The grain size determined by x-ray diffraction remained constant. However, the residual resistivity increased by a factor of 1.5, possibly indicating rejection of a small quantity of Al₂O₃ to the grain boundaries.

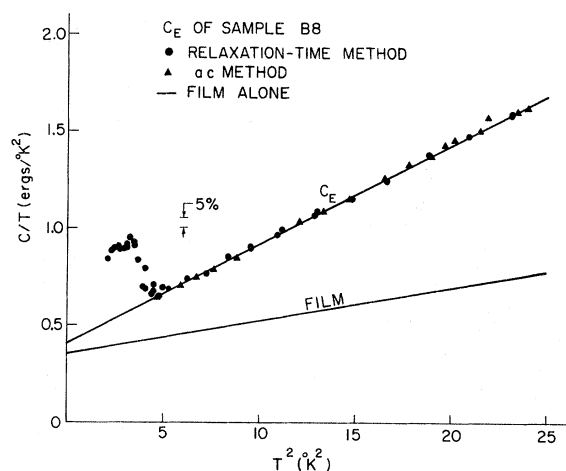


FIG. 5. Experimental heat capacity of film B8. Experimental points include the thermometer and wire fraction heat capacities. Correcting for this addendum gives the normal heat capacity of the film alone as shown by the line.

The heat capacity was practically unchanged indicating that the enhancement of T_c is stable with time.

To compare our results with the specific heat of pure aluminum the metallic Al content of the film must be known. In a previous report¹⁷ we used the sputtering target composition to calculate the molar values of γ and β . Since both the microprobe and chemical analyses give lower aluminum content for the film than the sputtering target, it appears that additional oxide forms throughout the film after preparation and our previous values of γ and β were incorrect. From the known characteristics of aluminum oxidation the oxide would form very quickly on exposure to air and then cease to grow further. The small grain size and film structure as shown in Fig. 4 may allow for oxide formation throughout the entire film rather than just at the surface. If it is assumed the film is composed of Al and Al_2O_3 (as it will be in equilibrium), the microprobe and chemical analyses give the metallic aluminum content as 65 ± 5 wt%. Using this value we compute the molar values of γ and β shown in Table II. The value of γ is, within experimental error, the same as the bulk Al value of 1.35 $\text{mJ}/^\circ\text{K mole}$.¹⁸ The value of β is larger than the β

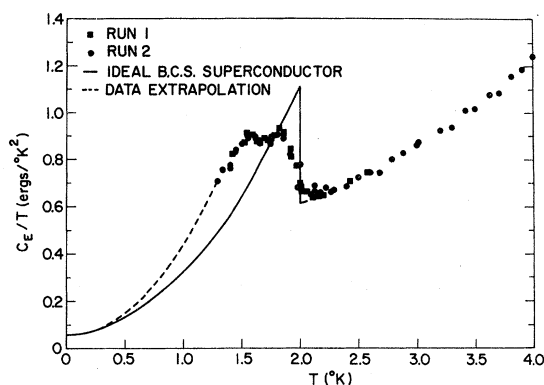


FIG. 6. Experimental heat capacity of film B8 in the superconducting transition region. The circles are from later measurements taken after the film was aged in air for three months at room temperature. The solid line represents the heat capacity of an ideal BCS superconductor with the same electronic heat-capacity coefficient as the sample and $T_c = 2.0$ $^\circ\text{K}$. The nonzero intercept at $T = 0$ is the result of nonsuperconducting addendum.

value for pure Al and corresponds to $\Theta_D = 306 \pm 15$ $^\circ\text{K}$, which is significantly smaller than the 428 $^\circ\text{K}$ Debye temperature of bulk Al.¹⁸ Some of this excess lattice heat capacity could be caused by the Al_2O_3 in the film. However, 0.30 mg of crystalline Al_2O_3 has a β of only 5×10^{-12} $\text{J}/^\circ\text{K}$. This cannot account for the decrease in Θ_D unless the amorphous Al_2O_3 in our film has ~ 100 times the heat capacity of crystalline Al_2O_3 .

In addition to the measurements made using the previously described silicon thermometers, the heat capacity of a free-standing granular Al film was also measured. This film was made by evaporation in the presence of a partial pressure of oxygen.¹⁹ The sample was a disc with a small gold spot evaporated on the center. The temperature of the sample was measured with a Au + 7 at.% Fe versus Cu thermocouple spot welded directly to the Au spot. To make an absolute measurement of the heat capacity, $P(\omega)$ must be known accurately. Since it was not possible to use an electrical heater on the sample, K_w could not be measured. Therefore, a comparison method was used to measure $P(\omega)$. The magnitude of the ac signal from an aluminum or copper reference sample mounted beside the film sample was used to cal-

TABLE II. Heat capacity of film B8.

Heat-capacity coefficients	First run C_E	Second run C_E	C_{Addendum}	C_{film} 1.057 mg	$C_{\text{per mole}}$ Aluminum
γ ($\text{J}/^\circ\text{K}^2$)	$4.1 \pm 0.1 \times 10^{-8}$	$4.0 \pm 0.1 \times 10^{-8}$	$0.6 \pm 0.2 \times 10^{-8}$	$3.5 \pm 0.2 \times 10^{-8}$	$1.37 \pm 0.1 \times 10^{-3}$
β ($\text{J}/^\circ\text{K}^4$)	$5.1 \pm 0.15 \times 10^{-9}$	$5.3 \pm 0.15 \times 10^{-9}$	$3.38 \pm 0.1 \times 10^{-9}$	$1.7_2 \pm 0.2 \times 10^{-9}$	$68 \pm 9 \times 10^{-6}$
δ ($\text{J}/^\circ\text{K}^6$)	$5.3 \pm 10 \times 10^{-13}$	$5.2 \pm 1 \times 10^{-12}$	7.8×10^{-13}

culate $P(\omega)$ [Eq. (3)].

Experimentally, it was difficult to obtain a proper normalization because of τ_2 effects. The poor thermal conductivity of our granular films produced a temperature gradient between the edge and the center of the sample. This effect is eliminated when the film is on a high thermal conductivity substrate such as our silicon thermometers. Because of this normalization problem, the thermocouple method was not satisfactory for obtaining absolute values of heat capacity. Consequently, the γ/β ratio for sample 24A is listed in Table III, since it is independent of normalization. The γ/β ratio for a pure Al foil was also measured. This compared well with the γ/β ratio measured for pure Al by Phillips.¹⁸ Table III also contains the Debye temperature of sample 24A calculated with the assumption that the electronic density of states is unchanged from pure Al. The results on the free-standing film are quite similar to those of sample B8 discussed above.

V. DISCUSSION

Several experiments^{2,20,21} have shown that the residual resistivity ρ_0 of Al-Al₂O₃ films, deposited at room temperature, correlates well with T_c . This correlation was valid for films ranging in thickness from 100 Å to 6 μm. Both residual resistivity and the superconducting T_c of the 25-μm-thick heat-capacity films are lower than those of thinner films prepared in the same manner ($\rho_0 \approx 1000 \mu\Omega \text{ cm}$, $T_c \approx 2.45 \text{ °K}$). However, the ρ_0 and T_c of these thick films fall on the same curve of T_c versus ρ_0 as do the thinner films. This indicates that our films are good prototypes of the Al-Al₂O₃ system.

The x rays and scanning electron micrographs indicate that film B8 is inhomogeneous with large grains at the surface and smaller grains ($\leq 100 \text{ Å}$) within the film. It is possible that grain sizes in the thick films range from 50 to 100 Å reported previously^{2,20} for granular Al films to 5000 Å at the surface.²² This inhomogeneity is quite evident in the heat-capacity data. It shows up as a rather

broad superconducting transition stretching from 2 down to 1.6 °K. The larger average grain size also correlates with the smaller value of T_c enhancement of the thick films as compared with a thin film.

The experimental accuracy in the quantitative determination of the electronic heat-capacity coefficient γ is only 10% because of the addendum and film composition uncertainties. Within this accuracy γ has the same value as that of bulk aluminum. According to McMillan's theory of strong-coupling superconductors,³ the electronic heat-capacity coefficient is larger than the band-structure value by the factor $(1+\lambda)$, i. e.,

$$\gamma = \gamma_{\text{bs}}(1+\lambda), \quad (8)$$

where λ is the electron-phonon coupling parameter. For the enhancement of T_c we observe that this theory would predict an increase in λ by $\sim 10\%$ over that of bulk aluminum. Theoretically, it is not clear how the value of γ_{bs} for granular Al should compare with that of bulk aluminum. If the only significant change from bulk aluminum is a 1.5% volume expansion, free-electron theory would predict a 1% larger γ_{bs} for granular aluminum from the relation

$$\frac{\Delta N(E_F)}{N(E_F)} = \frac{2}{3} \frac{\Delta V}{V}. \quad (9)$$

Recent theoretical calculations predict small size metallic particles should have smaller electronic heat capacity.²³ The difference is roughly 3% at 3 °K for 100-Å particles and varies as $1/L^3$, where L is the particle dimension. However, it is not clear that the grains in our films are isolated sufficiently electrically for this calculation to apply. The value of γ_{bs} may also be modified by the presence of Al₂O₃ in the grains.

From the above considerations it seems that the γ of granular aluminum should be within 10% of that of bulk aluminum. Our data fall within this range with the observed value of 1.37 mJ/mole °K being 2% above the bulk value. However, the uncertainty of film composition and addendum correction makes

TABLE III. Measured properties of Al foil A, film 24A, and film B8.

Sample	Composition	γ/β	Θ_D (°K)	T_c (°K) determined by		Mass (mg)
			assuming bulk γ	Resistivity	Specific Heat ^a	
A	100% Al	53.5 ± 0.5	418	1.2	1.2	5.06
24A	79% Al 21% Al ₂ O ₃	18.5 ± 0.5	300	1.85	1.9	1.640
B8	65% Al 35% Al ₂ O ₃	20.1 ± 1	306	2.06	2.0	1.057

^aSpecific heat T_c is defined as the temperature corresponding to the midpoint of the jump in C .

it difficult to attach significance to γ being slightly larger than that of bulk aluminum.

The low value of Θ_D of the granular aluminum film is the major difference in our data from that of bulk aluminum. Many authors have suggested that lower phonon frequencies in granular films were responsible for their increased T_c . These suggestions are based on McMillan's theory of strong-coupled superconductors.³ McMillan showed that the electron-phonon interaction parameter λ can be written

$$\lambda = \frac{N(0)\langle I^2 \rangle}{M\langle \omega^2 \rangle}, \quad (10)$$

where $N(0)$ is the electron density of states at the Fermi surface, $\langle I^2 \rangle$ is the average over the Fermi surface of the square of the electronic matrix element, M is the atomic mass, and $\langle \omega^2 \rangle$ is a particular average of ω^2 over the phonon spectrum. Empirically McMillan found that $N(0)\langle I^2 \rangle = \text{const}$ for groups of related materials. Therefore, λ was mainly a function of $\langle \omega^2 \rangle$.

Our results are in qualitative agreement with McMillan in that the smaller Θ_D of our granular Al film implies a lower value of $\langle \omega^2 \rangle$ and thus increased values of λ and T_c over those of bulk aluminum. However, if one assumes $\lambda \propto 1/\Theta_D^2$ and uses McMillan's relation for the superconducting transition temperature

$$T_c = \frac{\Theta_D}{1.45} \exp\left(\frac{-1.04(1+\lambda)}{\lambda - \mu^*(1+0.62\lambda)}\right), \quad (11)$$

with $\mu^* = 0.1$ and $\lambda = 0.39$ for bulk Al,³ one finds that an 8% decrease in Θ_D is required to enhance T_c from 1.19 to 2 °K. The observed decrease in Θ_D was 28% for a granular film with $T_c = 2$ °K.

There is good reason to expect that the measured Θ_D cannot be directly used to calculate T_c . McMillan's $\langle \omega^2 \rangle$ is defined by an integral over the entire phonon spectrum

$$\langle \omega^2 \rangle = \int \left(\frac{d\omega}{\omega}\right) \omega^2 \alpha^2(\omega) f(\omega) / \int \left(\frac{d\omega}{\omega}\right) \alpha^2(\omega) f(\omega), \quad (12)$$

where $\alpha^2(\omega)$ is the energy-dependent electron-phonon coupling parameter and $f(\omega)$ is the phonon density of states. The low-temperature heat capacity Θ_D measured only the low-frequency part of $f(\omega)$, whereas the above integrals are dominated by the high-frequency part of $f(\omega)$ where the phonon density of states is largest. Thus, a change in Θ_D is not necessarily proportional to a change in $\langle \omega^2 \rangle^{1/2}$.

There are several possible ways in which Θ_D could decrease. In one extreme the entire phonon spectrum shifts down in frequency. In this case the ratio of Θ_D to $\langle \omega^2 \rangle^{1/2}$ is constant, and McMillan's formula should apply with $\lambda \propto 1/\Theta_D^2$. Our experimental results argue against this hypothesis.

Furthermore, a 27% shift in the entire phonon spectrum of Al is hard to imagine. If this were related to a volume change with a Grüneisen constant of 2, a 13.5% volume expansion would occur. Aluminum undergoes only a 6.5% volume change when melting and the observed volume expansion was only 1.5% for film B8.

A more probable explanation of the decrease in Θ_D is that the phonon spectrum has distorted such that $f(\omega)$ is larger than that of bulk aluminum at small ω . In this case the ratio of Θ_D to $\langle \omega^2 \rangle^{1/2}$ would be different; therefore, λ would not be proportional to $1/\Theta_D^2$, and T_c could not be calculated from Θ_D and Eq. (11).

Our measured decrease in Θ_D does seem to be in reasonable agreement with tunneling experiments, although the quantity measured in those experiments is $\alpha^2(\omega)f(\omega)$ and not $f(\omega)$ directly. For Al-Al₂O₃ granular films $\alpha^2(\omega)f(\omega)$ is larger at low frequency and smaller at high frequency than $\alpha^2(\omega)f(\omega)$ of pure Al.⁴ Similar results have been found for Pb, Sn,²⁴ Bi, and Ga²⁵ quench-condensed films, although this distortion was not found in Al-Ge films.²⁶

Recently, Ewert^{6,27} and Novotny *et al.*²⁸ have measured the heat capacity of granular Pb films at low temperature. Novotny *et al.* find an increased lattice heat capacity whereas Ewert finds that Θ_D is unaltered from the bulk value. Ewert reconciles his result with changes observed in $\alpha^2(\omega)f(\omega)$ via tunneling by concluding that $\alpha^2(\omega)$ alone must be altered in granular Pb. In contrast our results indicate $f(\omega)$ is changed for granular films, at least for the Al-Al₂O₃ system.

There have been several theoretical studies of the phonon spectrum of small particles and surface atoms of thin films.²⁹⁻³¹ While these studies do not directly apply to our granular Al-Al₂O₃ films, they indicate what changes to expect in the properties of surface atoms. These calculations show that surface atoms are bound by weaker forces because of missing neighbors. This leads to surface atoms having lower frequencies and larger amplitudes of vibration than atoms in the interior of the grains. The frequencies of these "surface modes" are usually slightly below the transverse acoustical modes and about one-half of the longitudinal acoustical modes. The presence of surface modes causes a downward energy shift in the phonon spectrum and also increases $f(\omega)$ at small ω and decreases $f(\omega)$ at large ω . If the entire phonon spectrum were measured, both a distortion and a shift of the phonon densities would be observed.

Presumably our granular Al films have an Al-Al₂O₃ interface at the grain boundaries. If this mismatch in chemical bonds causes weaker force constants for the surface Al atoms, they would behave qualitatively like free surface atoms men-

tioned above. In order to see these surface modes in heat-capacity measurements the fraction of atoms near surface would have to be large. For films with grain size of 100 Å, approximately 30% of the atoms would be within 5 Å of the surface of grains, which is indeed a significant fraction of the Al atoms. We believe that our measured enhancement in lattice specific heat is evidence for these soft surface modes.

VI. SUMMARY

We have discussed techniques to measure low-temperature absolute heat capacities of magnitude ~ 0.5 erg/°K. The addendum correction was minimized by using a low-heat-capacity silicon resistance thermometer as the sample substrate and laser light to heat the sample. Calculations of the addendum corrections due to the electrical lead wires were presented. Data on the thermal conductivity of Au+7-at.%-Cu wires and the heat capacity of a silicon resistance thermometer were given as examples of the capabilities and accuracy of the method.

The specific heat of granular Al-Al₂O₃ films with $T_c \cong 2$ °K has been measured. The data show that the enhancement of T_c is a bulk effect. Within experimental accuracy (10%) the electron density of states at the Fermi surface is the same as that

of pure Al. A definite increase in the low-temperature lattice heat capacity of granular Al-Al₂O₃ over that of pure aluminum was measured. Qualitatively this is in agreement with the "soft mode" theory of enhanced T_c in granular films. Our data indicate that the phonon density of states is enhanced at low frequencies, a result which is consistent with the tunneling data of Leger and Klein.⁴

Note added in proof. Recently, Happle, Knorr, and Barth³² have compared tunneling and specific-heat data for disordered Pb and Pb-Bi films. They conclude that $f(\omega)$ is enhanced at low-frequencies in these systems in agreement with our conclusions about $f(\omega)$ in the granular Al system.

ACKNOWLEDGMENTS

It is a pleasure to thank Professors T. H. Geballe and W. A. Phillips for many stimulating discussions and much encouragement during the course of this work. We thank Professor J. A. Krumhansl for critical discussions of our results. The technical assistance of H.-U. Thomas and F. Futterer is greatly appreciated. We wish to thank N. E. Phillips for kindly furnishing us with a calibrated Ge thermometer, George Martin for technical help with the microprobe, Dr. David Kyser for an independent microprobe analysis, and Erich Meier for the chemical analysis.

*Research sponsored by the U. S. Air Force Office of Scientific Research under Grant No. AFOSR 68-1510C.

†Present address: IBM Research Laboratory, Dept. K03, San Jose, Calif. 95114.

¹W. Buckel and R. Hilsch, Z. Physik **138**, 109 (1954).

²The experimental and theoretical studies pertinent to enhanced superconductivity have been discussed by J. J. Hauser, Phys. Rev. B **3**, 1611 (1971).

³W. L. McMillan, Phys. Rev. **167**, 331 (1968).

⁴A. Leger and J. Klein, Phys. Letters **28A**, 751 (1969).

⁵R. Watton [Solid State Commun. **8**, 105 (1970)] has found surface modes can explain his resistivity results.

⁶Recently, S. Ewert [Z. Physik **237**, 47 (1970)] has measured the specific heat of other granular and amorphous films.

⁷J. J. Hauser [J. Low Temp. Phys. **7**, 335 (1972)] has measured the susceptibility and NMR of some granular Al films. This work and our specific-heat work are the first truly bulk measurements on granular Al films.

⁸G. D. Zally and J. M. Mochel [Phys. Rev. Letters **27**, 1710 (1971)] have measured a sample with heat capacity similar to ours, but they did not separate the contribution of the addendum from the sample.

⁹R. Bachmann *et al.*, Rev. Sci. Instr. **43**, 205 (1972).

¹⁰P. F. Sullivan and G. Seidel, Phys. Rev. **173**, 679 (1968).

¹¹Corning filter 1-69.

¹²C. N. King, Ph.D. dissertation (Stanford University, 1972) (unpublished).

¹³Wire was purchased from California Fine Wire Co., Grover City, Calif.

¹⁴P. G. Klemens, G. K. White, and R. J. Tainsh, Phil. Mag. **7**, 1323 (1962).

¹⁵P. Flubacher, A. J. Leadbetter, and J. A. Morrison, Phil. Mag. **4**, 273 (1959).

¹⁶R. A. Chalmers and M. A. Basit, Analyst **92**, 680 (1967).

¹⁷R. L. Greene, C. N. King, and R. B. Zubeck, Bull. Am. Phys. Soc. **16**, 850 (1971).

¹⁸N. E. Phillips, Phys. Rev. **114**, 676 (1959).

¹⁹B. Abeles, R. W. Cohen, and G. W. Cullen, Phys. Rev. Letters **17**, 632 (1966).

²⁰R. W. Cohen and B. Abeles, Phys. Rev. **168**, 444 (1968).

²¹W. E. Masker and R. D. Parks, Phys. Rev. B **1**, 2164 (1970).

²²It was found that the sputtering target becomes Al rich for lengthy evaporations. This would lead to larger grain size at the top surface of the film.

²³R. Denton, B. Muhlschlegel, and D. J. Scalapino, Phys. Rev. Letters **26**, 707 (1971).

²⁴K. Knorr and N. Barth, Solid State Commun. **8**, 1085 (1970).

²⁵T. T. Chen, J. T. Chen, J. D. Leslie, and H. J. T. Smith, Phys. Rev. Letters **22**, 526 (1969).

²⁶G. Deutscher, J. P. Farges, F. Meunier, and P. Nedeller, Phys. Letters **35A**, 265 (1971).

²⁷S. Ewert and W. Sander, Z. Physik **247**, 21 (1971).

²⁸V. Novotny, P. P. M. Meincke, and J. H. P. Watson, Phys. Rev. Letters **28**, 901 (1972).

²⁹J. M. Dickey and A. Paskin, Phys. Rev. Letters **21**, 1441 (1968).

³⁰F. W. De Wette and R. E. Allen, Phys. Rev. **187**, 878 (1969).

883 (1969).

³¹R. E. Allen and F. W. De Wette, Phys. Rev. **187**,

³²H. Happel, K. Knorr, and N. Barth, Z. Physik **249**, 185 (1971).

PHYSICAL REVIEW B

VOLUME 6, NUMBER 9

1 NOVEMBER 1972

Hall Effect in the Hubbard Model: Low-Field Regime*

M. L. Malwah and R. W. Bene'

Department of Electrical Engineering and Electronics Research Center, The University of Texas at Austin, Austin, Texas 78712

(Received 16 August 1971; revised manuscript received 15 May 1972)

The ac Hall conductivity in the Hubbard model has been calculated in the low-field large-correlation limit. It was found that the lowest order in the bandwidth for which the Hall conductivity is finite is second. The results of the second-order bandwidth calculation are then applied to a three-dimensional tight-binding model at $T=0^\circ\text{K}$ with the result that the Hall conductivity vanishes just where the diagonal components of the conductivity tensor do—for a half-filled band. The Hall and drift mobilities are then calculated for this model for $T \neq 0^\circ\text{K}$ for the half-filled band. The drift mobility has an exponential temperature dependence, while the Hall mobility remains equal to zero to second order in bandwidth. The calculations assume that the frequency is greater than the bandwidth.

I. INTRODUCTION

The motivation for much of the present interest in studying (both theoretically and experimentally) the properties of electrons in narrow bands is due to at least two reasons. First and probably foremost, from a theoretical point of view, one wishes to understand something of the intermediate cases between the insulator described by a Heitler-London model and wide-band metals described by single-electron bands. Second, however, there is also an immediate practical engineering reason for experimental work on many materials for which narrow bands play a major role. As has been pointed out,¹ there is a class of systems which has a much higher incidence than normal of materials which exhibit phase transitions of various sorts. This is the class of transition-metal oxides, sulfides, selenides, and tellurides. The common denominator of these materials is that they have narrow d bands, the width of which often dominates the electrical and magnetic properties. Thus, in these materials the properties of electrons in narrow bands are intimately tied to their properties near critical transition points.

The utilization of transition-point behavior in devices has been steadily gaining in importance in the last three or four years and promises to play a prominent role in device technology in the future. Examples of such utilization are superconducting bolometers,² pyroelectric detectors,³ pyromagnetic

detectors,⁴ and integrated inductors.⁵

There have appeared calculations for Hall effects in narrow-band models in the literature, notably the calculations of Holstein and Friedman⁶ using a small polaron model, and Langreth's derivation of an expression for the high-field Hall effect in the Hubbard model.⁷ In this paper, we derive the complement to Langreth's derivation, namely, the low-field Hall effect in the Hubbard model, and examine our results for the three-dimensional tight-binding model.

The general expression is derived in Sec. II using the nomenclature and general method used by Bari *et al.*⁸ in calculating the conductivity in this model. We do this calculation in the large-correlation limit. In Sec. III, we apply the results of Sec. II to a specific model, the three-dimensional tight-binding model at $T=0^\circ\text{K}$. In Sec. IV, we calculate the temperature dependence of the Hall and drift mobilities at the value of n (average number of electrons per atom) where the mobility vanishes at $T=0^\circ\text{K}$.

II. CALCULATION OF σ_{xy}^a

For a single narrow band, in the absence of external fields, Hubbard's⁹ Hamiltonian is given by

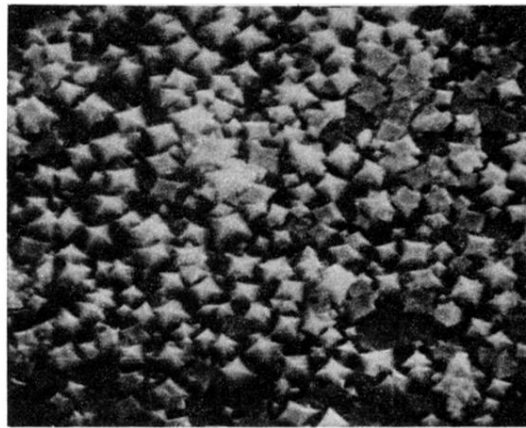
$$H_0' = \sum_{ij\sigma} T_{ij} C_{i\sigma}^\dagger C_{j\sigma} + \frac{1}{2} I \sum_{i\sigma} n_{i\sigma} n_{i-\sigma}, \quad (1)$$

where

$$T_{ij} = (1/N) \sum_{\mathbf{k}} \epsilon(\mathbf{k}) e^{i\mathbf{k} \cdot (\mathbf{R}_i - \mathbf{R}_j)} \quad (2)$$

and

$$I = e^2 \int \frac{\phi^*(\vec{\mathbf{R}} - \vec{\mathbf{R}}_i) \phi(\vec{\mathbf{R}} - \vec{\mathbf{R}}_i) \phi^*(\vec{\mathbf{R}}' - \vec{\mathbf{R}}_i) \phi(\vec{\mathbf{R}}' - \vec{\mathbf{R}}_i) d\vec{\mathbf{R}} d\vec{\mathbf{R}}'}{|\vec{\mathbf{R}} - \vec{\mathbf{R}}'|}.$$



1μ

FIG. 4. Scanning electron micrograph of sample surface of film B8 as deposited. Magnification is 9000 \times .